

The European Large Area ISO Survey IV: the preliminary $90\mu\text{m}$ luminosity function

S. Serjeant¹, A. Efstathiou¹, S. Oliver^{1,2}, C. Surace¹, P. Heraudeau³,
M. Linden-Vørnle⁴, C. Gruppioni⁵, F. La Franca⁶, D. Rigopoulou⁷,
T. Morel¹, H. Crockett¹, T. Sumner¹, M. Rowan-Robinson¹, M. Graham¹

¹ *Astrophysics Group, Blackett Laboratory, Imperial College, Prince Consort Road, London SW7 2BW, UK*

² *Astronomy Centre, CPES, University of Sussex, Falmer, Brighton BN1 9QJ*

³ *Max-Planck-Institut für Astronomie, Königstuhl 17, D69117, Heidelberg, Germany*

⁴ *Danish Space Research Institute, 30 Juliane Maries Vej, DK-2100 Copenhagen 0, Denmark*

⁵ *Osservatorio Astronomico di Bologna, via Ranzani 1, 40127 Bologna, ITALY*

⁶ *Dipartimento di Fisica E. Amaldi, Via della Visca Navale 84, Rome, Italy*

⁷ *Max-Planck-Institut für extraterrestrische Physik Giessenbachstraße, 85748 Garching, Germany*

Accepted; Received; in original form 2000 Jun 19

ABSTRACT

We present the luminosity function of $90\mu\text{m}$ selected galaxies from the European Large Area ISO Survey (ELAIS), extending to $z = 0.3$. Their luminosities are in the range $10^9 < h_{65}^{-2} L/L_{\odot} < 10^{12}$, i.e. non-ultraluminous. From our sample of 37 reliably detected galaxies in the ELAIS S1 region from the Efstathiou et al. (2000) $S_{90} \geq 100\text{mJy}$ database, we found optical, $15\mu\text{m}$ or 1.4GHz identifications for 24 (65%). We have obtained 2dF and UK Schmidt FLAIR spectroscopy of 89% of IDs to rigid multivariate flux limits. We construct a luminosity function assuming (a) our spectroscopic subset is an unbiased sparse sample, and (b) there are no galaxies which would not be represented in our spectroscopic sample at *any* redshift. We argue that we can be confident of both assumptions. We find the luminosity function is well-described by the local $100\mu\text{m}$ luminosity function of Rowan-Robinson, Helou & Walker (1987). *Assuming* this local normalisation, we derive luminosity evolution of $(1+z)^{2.45 \pm 0.85}$ (95% confidence). We argue that star formation dominates the bolometric luminosities of these galaxies and we derive comoving star formation rates in broad agreement with the Flores et al. (1999) and Rowan-Robinson et al. (1997) mid-IR-based estimates.

Key words: cosmology: observations - galaxies: formation - infrared: galaxies - surveys - galaxies: evolution - galaxies: star-burst

1 INTRODUCTION

The study of the star formation history of the Universe is an extremely active field, in which much of the current debate is centred on the uncertainties in dust obscuration. Selecting star forming galaxies in the UV is relatively cheap in observing time, but such selection makes the samples extremely sensitive to dust obscuration. Detecting the reprocessed

starlight requires sub-mm surveys (e.g. Smail, Ivison & Blain 1997; Hughes et al. 1998; Barger et al. 1998, 1999; Eales et al. 1999, Peacock et al. 2000; Ivison et al. 2000a,b, Dunne et al. 2000) and/or space-based mid-far-IR surveys (e.g. Rowan-Robinson et al. 1997, Taniguchi et al. 1997, Kawara et al. 1998, Flores et al. 1999, Puget et al. 1999, Oliver et al. 2000; see e.g. Oliver 2000 for a review). As such, the European Large Area ISO Survey (ELAIS) is well-placed for

the study of the evolution and obscuration of the star formation in the Universe, and strong constraints at $z \lesssim 1$ are possible from ELAIS (Oliver et al. 2000).

The scientific aims and strategy of ELAIS are presented in detail in Paper I (Oliver et al. 2000). In Papers II and III (Serjeant et al. 2000, Efstathiou et al. 2000) we presented respectively the ELAIS Preliminary Analysis source counts from the CAM ($6.7\mu\text{m}$ and $15\mu\text{m}$) and PHOT ($90\mu\text{m}$) instruments on ISO. The $90\mu\text{m}$ sample covered 11.6 square degrees, and the source counts were found to agree well at the bright end with the IRAS $100\mu\text{m}$ counts. Excellent agreement was also achieved with a parallel independent pipeline (Surace et al. in prep.).

In this paper we present the first $90\mu\text{m}$ luminosity function from our initial spectroscopic campaigns in the ELAIS S1 field (Oliver et al. 2000 in prep., Gruppioni et al. 2000 in prep., La Franca et al. 2000 in prep., Linden-Vørnle et al. 2000 in prep.). Section 2 defines our sample. In section 3 we use this catalogue to derive a $90\mu\text{m}$ luminosity function. We discuss the implications of our results in section 4. We assume $H_0 = 65 \text{ km s}^{-1} \text{ Mpc}^{-1}$, $\Omega_0 = 1$, $\Lambda = 0$ throughout.

2 SAMPLE SELECTION AND DATA ACQUISITION

The parent sample for this study is the Preliminary Analysis catalogue of Efstathiou et al. 2000 (Paper III), with $90\mu\text{m}$ fluxes satisfying $S_{90} > 100\text{mJy}$. The completeness of this sample falls approaching this limit but has been well-quantified with simulations (figure 6 of Paper III). We will use the calibration adopted in Paper III. The $90\mu\text{m}$ flux calibration is still uncertain to within $\sim 30\%$, as discussed in Paper III; however, in order to be consistent with the $100\mu\text{m}$ IRAS source counts (assuming $S_{90} \simeq S_{100}$) the flux calibration has to be very close to the Paper III value. Therefore when we compare our $90\mu\text{m}$ luminosity function to the local $100\mu\text{m}$ luminosity function below, we will treat the flux calibration as being accurately known. Nevertheless, in predicting the redshift distributions of other $90\mu\text{m}$ surveys, we will not neglect the flux calibration systematics.

We restrict our study to the ELAIS S1 field with $90\mu\text{m}$, 1.4GHz and $15\mu\text{m}$ survey coverage, which covers 3.96 square degrees and has the most extensive available optical spectroscopy. Large-scale-structure variations are negligible in the comoving volume of the total ELAIS survey, but the ELAIS S1 field has slightly lower source counts than the global average. Consequently we reduced the effective area by 20% (a factor of 0.8) to make the S1 counts normalisation match the whole survey, to account for any possible large scale structure fluctuations. (This correction is smaller than the errors in the luminosity function derived below.) We sought identifications of this sample using (a) the APM (Automatic Plate Measuring ma-

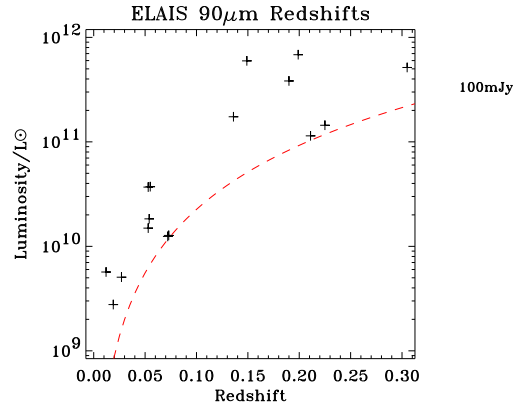


Figure 1. Luminosity - redshift plane. The 100mJy flux limit is marked.

chine), (b) sub-mJy decimetric radio sources from our Australia Telescope Compact Array (ATCA) imaging (Gruppioni et al. 1999), (c) our ELAIS ISOCAM $6.7\mu\text{m}$ and $15\mu\text{m}$ catalogues (Serjeant et al. 2000, Paper II). By randomising our 37 catalogue positions in the cross-correlation, we found that < 1 optical APM identifications brighter than $R = 17$ should occur by chance within the error ellipses of all our PHOT sources, and similarly restricted the association radius for the CAM and radio catalogues. Optical spectroscopy was obtained at the 2 degree field (2dF) at the Anglo-Australian Telescope (AAT), the Fibre Linked Array Image Reformatter (FLAIR) spectrograph at the UK Schmidt and with the Danish Faint Object Spectrograph and Camera (DFOSC) at the Danish 1.54m at ESO. The optical spectroscopic catalogue will appear in future papers in this series. Of the 37 reliably detected galaxies, 24 had multi-wavelength identifications of which 18 are above the combined multivariate flux limits discussed above. Of these we have obtained optical spectroscopy of 89%. The ELAIS S1 $90\mu\text{m}$ sample is presented in table 1 with the cross-identifications and available redshifts. This table also lists redshifts for four identifications for which the identification is uncertain. These galaxies fail the strict selection function defined below and are excluded from the luminosity function analysis below. Two galaxies (ELAISP90_J003721-434228 and ELAISP90_J003021-423657) are Seyfert II galaxies and two further galaxies (ELAISP90_J003431-433806 and ELAISP90_J003133-425100) have an early type spectrum; all the remainder (including the four excluded identifications) show starburst emission line spectra.

3 RESULTS: THE 90 MICRON LUMINOSITY FUNCTION

Our selection function is as follows. In order to be in the spectroscopic target list, a $90\mu\text{m}$ galaxy must either have (a) a reliable optical identification brighter

Name	RA (J2000)	Dec (J2000)	S_{90} /Jy	S_{15} /mJy	$S_{1.4}$ /mJy	R	z	z_{\max}	L/L_{\odot}
ELAISP90_J003857-424358	00 38 57.7	-42 43 58.8	0.43	2.9	0.964				
ELAISP90_J003056-441633	00 30 57.0	-44 16 33.6	0.35	4.9		13.7	0.019	0.0351 ^P	2.8×10^9
ELAISP90_J003510-435906	00 35 10.5	-43 59 6.0	0.41	9.6		12.1	0.136	0.272 ^P	1.7×10^{11}
ELAISP90_J003431-432613	00 34 31.6	-43 26 13.2	0.59			14.0	0.053	0.127 ^P	3.7×10^{10}
ELAISP90_J003914-430437	00 39 14.8	-43 04 37.2	1.79	16.2		11.6	0.012	0.049 ^P	5.7×10^9
ELAISP90_J003021-423657	00 30 21.1	-42 36 57.6	1.17	22.3		16.0	0.149	0.493 ^P	6.0×10^{11}
ELAISP90_J003459-425718	00 34 59.0	-42 57 18.0	0.55	5.5	1.371	14.9	0.055	0.101 ^R	3.7×10^{10}
ELAISP90_J003134-424420	00 31 34.5	-42 44 20.4	0.31			13.1	0.027	0.048 ^P	5.1×10^9
ELAISP90_J003242-423314	00 32 42.9	-42 33 14.4	0.24	2.6	0.463	15.2	0.053	0.081 ^P	1.5×10^{10}
ELAISP90_J003615-424344	00 36 15.4	-42 43 44.4	0.31			17.2	0.115		
ELAISP90_J003516-440448	00 35 16.1	-44 04 48.0	0.29						
ELAISP90_J003741-440227	00 37 41.6	-44 02 27.6	0.21			19.9	0.348		
ELAISP90_J003431-433806	00 34 31.2	-43 38 6.0	0.75		0.595	18.4	0.199	0.357 ^O	6.8×10^{11}
ELAISP90_J003405-423816	00 34 5.3	-42 38 16.8	0.23						
ELAISP90_J003358-441102	00 33 58.2	-44 11 2.4	0.23	5.0		18.9	0.305	0.446 ^O	5.2×10^{11}
ELAISP90_J003501-423852	00 35 1.9	-42 38 52.8	0.28		0.606	15.9	0.054	0.090 ^P	1.8×10^{10}
ELAISP90_J003254-424608	00 32 54.2	-42 46 8.4	0.46	2.5	0.469	17.7	0.190	0.207 ^C	3.8×10^{11}
ELAISP90_J003531-423314	00 35 31.4	-42 33 14.4	0.16						
ELAISP90_J003635-430148	00 36 35.7	-43 01 48.0	0.12	4.5	0.358	21.5			
ELAISP90_J003019-432006	00 30 19.8	-43 20 6.0	0.20						
ELAISP90_J003839-422324	00 38 40.0	-42 23 24.0	0.14						
ELAISP90_J003014-440509	00 30 14.3	-44 05 9.6	0.10	3.6					
ELAISP90_J003912-431203	00 39 12.2	-43 12 3.6	0.15	5.0		14.8			
ELAISP90_J003133-425100	00 31 33.9	-42 51 0.0	0.11	6.3		18.0	0.211	0.222 ^P	1.1×10^{11}
ELAISP90_J003304-425212	00 33 4.3	-42 52 12.0	0.19	1.4		15.6			
ELAISP90_J003046-432204	00 30 46.4	-43 22 4.8	0.11	6.2		15.6	0.073	0.075 ^P	1.3×10^{10}
ELAISP90_J003027-433050	00 30 27.7	-43 30 50.4	0.11	4.9		15.7	0.072	0.074 ^P	1.2×10^{10}
ELAISP90_J002845-424420	00 28 45.5	-42 44 20.4	0.11						
ELAISP90_J003719-421955	00 37 19.4	-42 19 55.2	0.16						
ELAISP90_J003725-424554	00 37 25.2	-42 45 54.0	0.12						
ELAISP90_J003731-440758	00 37 31.3	-44 07 58.8	0.32			20.0			
ELAISP90_J003625-441127	00 36 25.0	-44 11 27.6	0.14		4.265				
ELAISP90_J003721-434228	00 37 21.5	-43 42 28.8	0.12	17.3	0.451	17.4	0.225	0.248 ^P	1.4×10^{11}
ELAISP90_J003348-433032	00 33 48.3	-43 30 32.4	0.15						
ELAISP90_J003149-423628	00 31 49.2	-42 36 28.8	0.11						
ELAISP90_J003244-424803	00 32 44.4	-42 48 3.6	0.12	1.2		19.0	0.192		
ELAISP90_J003323-432634	00 33 23.2	-43 26 34.8	0.19			18.7	0.316		

Table 1. ELAIS S1 90 μ m sample. The 90 μ m photometry has a $\sim 30\%$ possible systematic uncertainty (see Paper III), and the 15 μ m photometry is subject to a possible systematic scaling to fainter fluxes by up to a factor of ~ 1.5 (see Paper II). We assume $H_0 = 65 \text{ km s}^{-1} \text{ Mpc}^{-1}$, $\Omega_0 = 1$, $\Lambda = 0$, and bolometric luminosities are calculated at 90 μ m assuming a constant νL_{ν} spectrum. The maximum accessible redshifts z_{\max} quoted assume no evolution, and are labelled respectively as *P*, *R*, *O* and *C* for maximum redshifts imposed by the 90 μ m PHOT flux limit, the radio flux limit, the optical magnitude limit and the CAM flux limit. Two galaxies (ELAISP90_J003721-434228 and ELAISP90_J003021-423657) are Seyfert II galaxies and two further galaxies (ELAISP90_J003431-433806 and ELAISP90_J003133-425100) have an early type spectrum; all the remainder show starburst emission line spectra. Also listed are 4 redshifts for candidate optical IDs with the optical magnitudes listed, but which lack other multi-wavelength detections and are too faint optically to be certain that the correct ID has been found. All 4 such identifications show starburst emission line spectra, but nevertheless are excluded from the luminosity function analysis as they fail the strict selection function defined in the text.

than $R = 17$, or (b) a reliable 15 μ m or 1.4GHz identification, together with an optical ID brighter than $R = 20$. The 15 μ m identifications were made to $S_{15} \geq 2\text{mJy}$, and the radio identifications to $0.2 - 0.4\text{mJy}$ depending on position (Grupponi et al. 1999). Only 90 μ m galaxies in the area with radio and 15 μ m survey coverage were considered. We use the M82 starburst model from Rowan-Robinson et al. 1997 to estimate the K-corrections, with $S_{60\mu\text{m}} = 120S_{1.4\text{GHz}}$ and a radio spectral index of $d \log_{10} S / d \log_{10} \nu = -0.8$. For optical K-corrections we assume an optical spectral

index of -3 . The luminosity-redshift plane is shown in figure 1, with bolometric luminosities calculated at 90 μ m assuming constant νL_{ν} (for ease of conversion to other luminosity scales). Our method for calculating the luminosity function in the face of this complicated selection function is dealt with in the appendix. Note that our method relies on the underlying assumption that no galaxies are missing at *all* redshifts due to the multivariate flux limits. However, we can be confident of this in our case, as any sufficiently low-redshift galaxy will have an optical iden-

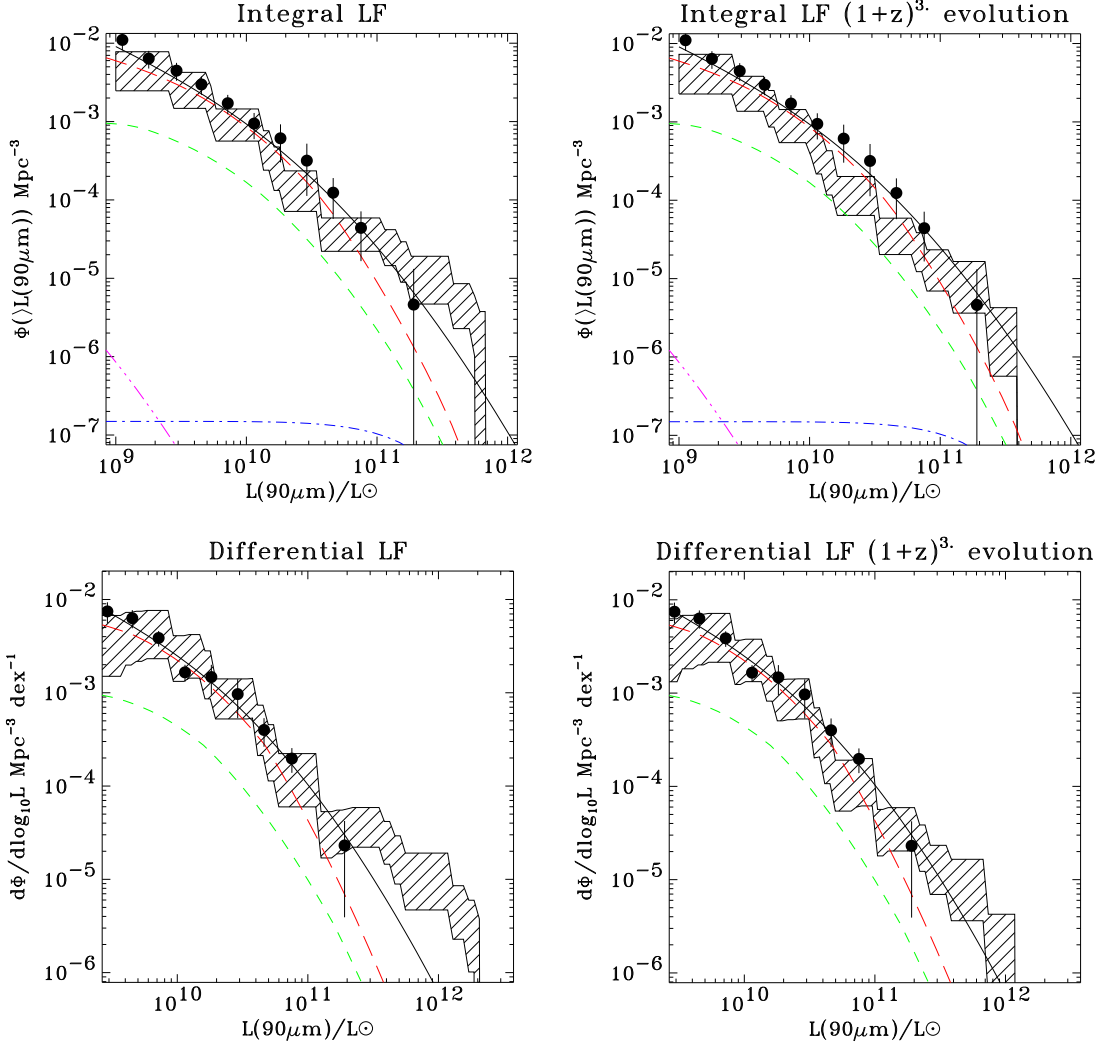


Figure 2. Luminosity function assuming no evolution (left) and $(1+z)^3$ luminosity evolution (right). Upper figures show the integral luminosity function, lower figures show the differential form. Shaded area is the $\pm 1\sigma$ error region from this study. For the differential counts, the shaded area indicates the error on the luminosity function in a ± 0.5 dex bin; the differential counts are therefore effectively smoothed by a 1 dex boxcar. The data points show the local $100\mu\text{m}$ luminosity function of Rowan–Robinson, Helou & Walker (1987), and the full line is a fit to this local data. The broken lines show the populations in the Rowan–Robinson (2000) model. The long dashed line is the “cirrus-like” population, i.e. galaxies with bolometric luminosities dominated by new stars heating previously-created dust. N.B., this population is not necessarily identified with NGC 6090-like cirrus galaxies. The short dashed line is the starburst population; dash-dot indicates Arp-220-like galaxies; dash-dot-dot-dot shows the AGN population.

tification that will pass criterion (a) of our selection function. A hypothetical local population of very optically faint but far-IR-bright galaxies can already be excluded from IRAS samples. We must also assume that our 89% complete optical spectroscopy is a random sparse sample of the total identifications (though not necessarily of the total $90\mu\text{m}$ sample). Although with our current spectroscopic sample this is an a posteriori selection rather than a priori, there were no selection biases in the spectroscopic data acquisition which could skew the sample selection function. We therefore correct our effective areal coverage by a

factor of 0.89 to account for the small optical spectroscopic incompleteness.

The integral luminosity function is given by

$$\Phi(> L) = \sum_{L_i > L} V_{\text{max},i}^{-1} \quad (1)$$

where the sum is performed over all objects having luminosities greater than L . In figure 2 we show this integral luminosity function, and compare it to the local $100\mu\text{m}$ luminosity function derived by Rowan–Robinson, Helou & Walker 1987 (binned data). The latter was derived from a sample in the north Galactic

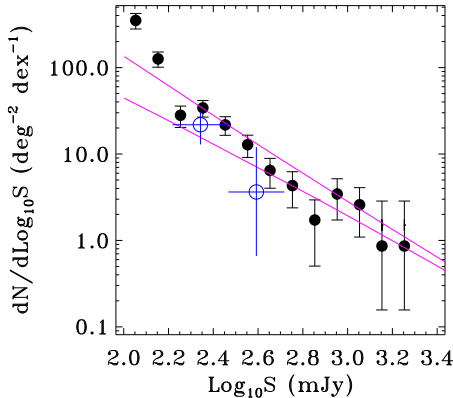


Figure 3. ELAIS source counts at 90 μ m, compared to a no-evolution model (shallow curve) and the $(1+z)^3$ luminosity evolution model (steeper curve). The no-evolution curve has a slightly shallower slope than its Euclidean equivalent. Also shown as open symbols are the Lockman Hole counts from Linden-Vørnle et al. (2000). All errors are Poissonian, except in the case of a single object in a bin for which the $\pm 1\sigma$ bounds on the number of objects in the bin are 0.18 – 3.3.

pole, and is subject to possible large scale structure variations. To estimate this, we compared the normalisation of their 60 μ m luminosity function with that of Saunders et al. (1990), and derived a correction factor of 0.77 to the normalisation of their 100 μ m luminosity function. The best-fit function to this local data is plotted as a full line. The adopted functional form is identical to Saunders et al. (1990):

$$\phi(L) = \phi_* \left(\frac{L}{L_*}\right)^{1-\alpha} \exp\left(-\frac{1}{2\sigma^2} \log^2\left(1 + \frac{L}{L_*}\right)\right) \quad (2)$$

and the best-fit parameters are given in table 2. Also plotted in this figure are the models of Rowan-Robinson (2000).

The shaded area shows the $\pm 1\sigma$ errors from our sample. There is a marginally significant excess at the highest luminosities. The $\langle V/V_{\max} \rangle$ statistic for this sample is 0.54 ± 0.07 ; a Kolmogorov-Smirnov test on the V/V_{\max} distribution shows only a 34% probability of inconsistency with the top-hat distribution $U[0, 1]$. Assuming $(1+z)^3$ luminosity evolution (figure 2) gives $\langle V/V_{\max} \rangle = 0.51 \pm 0.07$, and in both the evolving and non-evolving models, a Kolmogorov-Smirnov test on the observed luminosity distribution also gives acceptable confidence levels. Our spectroscopic sub-sample on its own is therefore not sufficiently large to reliably detect evolution.

A much stronger constraint on the strength of the evolution comes from the source counts slope. The 90 μ m counts in the entire ELAIS areas are significantly non-Euclidean (Paper III), but the counts do show a surprising upturn at the faintest end (figure 3). The cause of this upturn is not clear, but it is too large to be entirely attributable to uncertainties in the

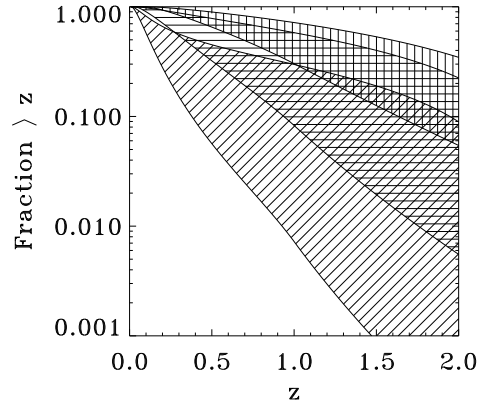


Figure 4. Predicted cumulative redshift distribution for surveys at 100 κ mJy (diagonal hatching), 10 κ mJy (horizontal hatching) and 1 κ mJy (vertical hatching), where $\kappa = 1 \pm 0.3$ indicates the uncertainty in the ELAIS PHOT absolute flux calibration. The bounds of the shaded areas are dominated by the assumed maximum redshift at which luminosity evolution occurs.

$\phi_* h_{65}^{-3}$	$\log_{10} L^* h_{65}^2 / L_{\odot}$	α
5.4 ± 1.8	9.67 ± 1.47	1.73 ± 0.04

Table 2. Best-fit parameters of the local luminosity function, with $\sigma = 0.724$ assumed. The reduced χ^2 of the best fit is 0.66.

completeness correction. One possibility is that some of the faintest sources are spurious glitch events, but all the sources have been eyeballed and accepted by at least two observers. Such a glitch population would have to be somewhat pathological. Evidence for comparably strong evolution at < 200 mJy in the Lockman Hole is also reported by Matsuhara et al. (2000) based on model fits to the fluctuations in their 90 μ m maps, consistent with the faintest ELAIS points. Nevertheless, in the absence of a clear model-independent interpretation, we confine our source count fits to the > 200 mJy region. We note that the sources used in the luminosity function are all reliably cross-identified at other wavelengths. The source counts at > 200 mJy are in good agreement with the Lockman Hole counts from Linden-Vørnle et al. 2000 (figure 3) who use a very different source extraction and flux calibration procedure to ELAIS. The ELAIS and Lockman counts for the faintest bin in figure 3 (165 – 294mJy) are 27 ± 4 and $22 \pm 9 \text{ deg}^{-2} \text{ dex}^{-1}$ respectively, and in the brightest bin (294 – 522 mJy) 19 ± 4 and $4_{-3.3}^{+9} \text{ deg}^{-2} \text{ dex}^{-1}$ respectively. Note that this represents only a single source in the Lockman Hole, so Poissonian errors would underestimate the error in this case. The $\pm 1\sigma$ bounds in the case of 1 observed source are 0.18 – 3.3, and all the remaining errors quoted in the counts are $\pm 1\sigma$ Poissonian errors.

If we *assume* the local luminosity function derived above undergoes $(1+z)^{\alpha}$ luminosity evolution we can obtain a constraint on the evolution param-

eter α . Note that this is relatively insensitive to the flux calibration uncertainty (Paper III). The correct relative normalisation between $90\mu\text{m}$ and $100\mu\text{m}$ for these purposes is one which achieves continuity in the source counts. The current $90\mu\text{m}$ calibration satisfies this almost exactly (Paper III) in that the bright end of the $90\mu\text{m}$ PHOT counts dovetail with the faint end of the $100\mu\text{m}$ IRAS counts, with little room for error in the *relative* calibration. The Kolmogorov-Smirnov test on the shape of the source counts yields a lower limit of $\alpha > 1.5$ at 95% confidence, and no-evolution models can be excluded at the 98% level. Stronger constraints still are possible if we include the normalisation of the source counts. Our goodness-of-fit statistic for this is $P_{\text{KS}} \times P_{\bar{N}}$, where P_{KS} is the significance level of rejecting the model of the shape of the source counts, and $P_{\bar{N}}$ is the significance level of rejecting the predicted normalisation. The distribution function for such statistics is quoted in e.g. Dunlop & Peacock 1990. We obtain $\alpha = 2.45 \pm 0.85$ (95% confidence). This is stronger than the constraint obtained purely from a V/V_{max} analysis of the spectroscopic sub-sample, partly because the number of galaxies comprising the source counts is much larger, partly also because we have assumed a fixed functional form for the zero redshift luminosity function, but mainly because we have set the $z = 0$ normalisation from IRAS.

4 DISCUSSION AND CONCLUSIONS

We have found that both the shape and normalisation of the $90\mu\text{m}$ luminosity function is well-described by the local luminosity function of Rowan-Robinson, Helou and Walker (1987), with evolution consistent with $(1+z)^{2.45 \pm 0.85}$ pure luminosity evolution, using the transformation $S_{100} \simeq S_{90}$. Pure density evolution is already excluded in this population as it conflicts with sub-mJy radio source counts (Rowan-Robinson et al. 1993).

We can use these results to predict the redshift ranges of current and future $90\mu\text{m}$ surveys. We assume the evolution extends to between $z = 1 - 2$ and is then unevolving. Figure 4 shows the 95% confidence limit for surveys of various depths, incorporating the uncertainty in the ELAIS $90\mu\text{m}$ absolute flux calibration. One corollary is that at least 10% of the currently unidentified $90\mu\text{m}$ galaxies in ELAIS extend to $z > 0.5$, possibly even $z > 2$.

Is it reasonable to assume that star formation dominates the bolometric luminosities of our $90\mu\text{m}$ sample? Genzel et al. (1998), Lutz et al. (1998) and Rigopoulou et al. (1999) have presented mid-infrared spectroscopy of ultraluminous galaxies ($L \geq 10^{12} L_{\odot}$) in the same redshift interval as our sample, and using the PAH features as a star formation indicator found that star formation dominates the bolometric power outputs in 70 – 80% of ULIRGs. The AGN bolomet-

ric fraction derived this way decreases monotonically at lower luminosities (e.g. Lutz et al. 1998). In local IR galaxies between 10^{11} and $10^{12} L_{\odot}$, $\sim 15\%$ have Seyfert II spectra (Telesco 1988), though care should be taken in interpreting AGN dominance from optical spectra (e.g. Lutz et al. 1999, Taniguchi et al. 1999). At $L < 10^{11} L_{\odot}$ most local IR galaxies are single, gas rich spirals (e.g. Sanders & Mirabel 1996) in which many lines of argument point to starburst dominance in the IR (e.g. Telesco 1988): for example, the similarity of the spectral energy distributions to those of galactic star forming regions; the linear $L_{\text{IR}} - L_{\text{CO}}$ correlation over many orders of magnitude in luminosity; and optical/IR spectroscopic confirmation of star formation activity. It therefore seems likely that our sub-ultraluminous population should not be powered by active nuclei, as is also suggested by the low fraction of spectra in our sample (10%) with Seyfert II features. (This does not imply that AGN activity cannot be present at a weak or bolometrically-neglectable level, e.g. Ho, Filippenko & Sargent 1997.) At the lowest luminosities there may be a significant contribution from cirrus which is at least partly illuminated by the old stellar population in the galaxies (Telesco 1988, Morel et al. 2000), though such galaxies nevertheless also still obey the starburst radio-far-IR relation (e.g. Condon 1992). We conclude that the galaxies in our sample have their bolometric luminosities dominated by star formation.

The Saunders et al. (1990) local luminosity density implies a local star formation rate of $0.023 \pm 0.002 M_{\odot} \text{ yr}^{-1} \text{ Mpc}^{-3}$ (Oliver et al. 1998) assuming a Salpeter initial mass function from $0.1 M_{\odot}$ to $125 M_{\odot}$. Our results imply this rises to $0.036 \pm 0.009 M_{\odot} \text{ yr}^{-1} \text{ Mpc}^{-3}$ by $z = 0.2$ (95% confidence), significantly higher than the Tresse & Maddox (1998) H α -based estimate of $0.022 \pm 0.007 M_{\odot} \text{ yr}^{-1} \text{ Mpc}^{-3}$. (Note that the two Seyfert II spectra in our sample are at the brightest end of the luminosity function where the contribution to the luminosity density is the smallest. The luminosity density is dominated by the galaxies around or below the break in table 2.) We believe this is due to two factors: firstly, the H α -based estimates are not immune to extinction effects, even if performing Balmer decrement reddening corrections (e.g. Serjeant, Gruppioni & Oliver 1998); secondly, the Tresse & Maddox (1998) survey area is sufficiently small to be affected by large-scale structure (e.g. Oliver, Gruppioni & Serjeant 1998). ELAIS is immune to these problems, as the cosmic variance over the PHOT survey area is $< 20\%$ at $z < 0.3$ (Paper I). These star formation rates are however consistent with extrapolations from those derived from mid-IR data at higher redshift by Flores et al. (1999) and Rowan-Robinson (1997).

The prospects for improving on the results presented here are excellent. A large-scale spectroscopic follow-up of the ELAIS northern areas is currently underway, which will have a major impact on the science

analysis of ELAIS. In particular, the ELAIS 15 μ m luminosity function will probe higher redshifts than accessible to PHOT at 90 μ m, from which the 15 μ m luminosity density can constrain the cosmic star formation history (e.g. Serjeant 2000).

ACKNOWLEDGEMENTS

We would like to thank Dave Clements and the anonymous referee for helpful comments on this paper. This work was supported by PPARC (grant number GR/K98728) and by the EC TMR Network programme (FMRX-CT96-0068).

APPENDIX: $1/V_{\text{MAX}}$ WITH MULTIVARIATE FLUX LIMITS

In a volume-limited non-evolving sample, the comoving number density of objects can be calculated trivially:

$$\phi = \frac{N}{V} = \frac{1}{V} \sum_{i=1}^N 1 \quad (3)$$

where V is the volume and N the number of objects. Suppose that the sample is incomplete in whatever way, and that the probability of the i^{th} object being contained in the sample is p_i . Provided that none of the p_i s in the underlying galaxy population are zero, the comoving number density in an observed sample of N_{obs} objects can be expressed as

$$\phi = \frac{1}{V} \sum_{i=1}^{N_{\text{obs}}} p_i^{-1}. \quad (4)$$

This will be an unbiased estimator of the underlying value.

Applying this formalism to our current data set, the incompleteness is due to the multivariate flux limits. We treat the (non-evolving) galaxies as sampling random redshifts within the volume, so that each p_i is the probability that such a galaxy would lie above the flux limits. The statement that the underlying p_i s are all non-zero is equivalent to assuming that there are no galaxies (in the 90 μ m luminosity range being considered) that would lie outside the selection criteria at all redshifts. We can be confident that this is the case, because any sufficiently local galaxy will have an optical identification passing criterion (a) of our selection function. A hypothetical population of FIR-luminous, optically-faint galaxies can already be excluded from IRAS.

There are two equivalent ways of calculating the p_i s. If we embed our flux-limited sample in a larger volume of size V_0 , we can use the assumption that the population is non-evolving and the fact that the flux limits are monotonic in z to express the p_i s as

$$p_i = \frac{V_{\text{max},i}}{V_0} \quad (5)$$

where $V_{\text{max},i}$ is the volume enclosed by the maximum redshift $z_{\text{max},i}$ at which the i^{th} object is visible. Note that this is the smallest redshift at which the object fails *any* of the selection criteria. The number density in a sample of N_{obs} galaxies is then

$$\phi = \frac{1}{V_0} \sum_{i=1}^{N_{\text{obs}}} \frac{V_0}{V_{\text{max},i}} = \sum_{i=1}^{N_{\text{obs}}} \frac{1}{V_{\text{max},i}}. \quad (6)$$

The RMS error is simply

$$\Delta\phi = \sqrt{\sum_{i=1}^{N_{\text{obs}}} \frac{1}{V_{\text{max},i}^2}}. \quad (7)$$

An alternative but equivalent method of calculating the p_i s is to model the incompleteness due to some or all of the multivariate flux limits by introducing a weighting factor to the differential volume elements:

$$dV' = \gamma(z, \dots)dV. \quad (8)$$

The $z_{\text{max},i}$ values would then be calculated using the remaining un-modelled flux limits only. If all the flux limits have been modelled, then $\forall i$ $z_{\text{max},i} = z_0$ where $V(z_0) = V_0$. The γ factor would drop to zero at some redshift if (under the previous method for calculating the $z_{\text{max},i}$) $z_0 > \max(z_{\text{max},i})$.

Here, our approach is to use the first method (equation 6) to treat the multi-variate flux limits, as it is less model-dependent. However we use a weighting function on the volume elements to correct for the ELAIS 90 μ m completeness function (figure 6 of Paper III):

$$V'_{\text{max},i} = \int_0^{z_{\text{max},i}} \gamma(z, S_i) \frac{dV}{dz} dz \quad (9)$$

where S_i is the 90 μ m flux of the i^{th} object.

To calculate the luminosity function in a redshift bin, an additional top-hat selection function is applied in redshift space and incorporated into the calculation of the $z_{\text{max},i}$. The volume enclosed by the minimum redshift of the bin must also be subtracted from the $V_{\text{max},i}$ in equation 5. We are currently confident that none of the underlying p_i s are zero, but if we calculated the luminosity function in a series of redshift bins this would not necessarily be the case for all bins. For example, there are galaxies in table 1 which only pass criterion (a) at the lowest redshifts, and these may be unobservable in principle in higher redshift bins. We would then need to make some model of the multi-variate correlations to correct for the missing $p_i=0$ galaxies. We therefore restrict ourselves to a single redshift range (de-evolving the galaxies if necessary), partly to avoid the model-dependence of correcting for missing populations, but partly also because of our small sample size.

REFERENCES

- Barger, A.J., Cowie, L.L., Sanders, D.B., Fulton, E., Taniguchi, Y., Sato, Y., Kawara, K., Okuda, H., 1998, *Nature*, 394, 248
- Barger, A., Cowie, L.L., Smail, I., Ivison, R.J., Blain, A.W., Kneib, J.-P., 1999, *AJ*, 117, 2656
- Condon J.J., 1992, *ARA&A*, 30, 575
- Dunlop, J.S., & Peacock, J.D., 1990, *MNRAS*, 247, 19
- Dunne, L., Eales, S., Edmunds, M., Ivison, R., Alexander, P., Clements, D.L., 2000, *MNRAS*, 315, 115
- Eales, S., Lilly, S., Gear, W., Dunne, L., Bond, J.R., Hammer, F., Le Fèvre, O., Crampton, D., 1999, *ApJ*, 515, 518
- Efstathiou, A., et al., 2000, *MNRAS* in press (Paper III)
- Flores, H., et al., 1999, *ApJ*, 517, 148
- Grupponi, C., et al., 1999, *MNRAS*, 305, 297
- Genzel, R., et al., 1998 *ApJ*, 498, 579
- Ho, L.C., Filippenko, A.V., Sargent, W.L.W., 1997, *ApJS*, 112, 315
- Hughes, D., Serjeant, S., Dunlop, J., Rowan-Robinson, M., Blain, A., Mann, R.G., Peacock, J., Efstathiou, A., Gear, W., Oliver, S., Lawrence, A., Longair, M., Goldschmidt, P., Jennes, T., 1998, *Nature*, 394, 421
- Ivison, R.J., Dunlop, J.S., Smail, I., Dey, A., Liu, M.C., Graham, J.R., 2000a, *ApJ*, in press (*astro-ph/0005234*)
- Ivison, R.J., Smail, I., Barger, A.J., Kneib, J.-P., Blain, A.W., Owen, F.N., Kerr, T.H., Cowie, L.L., *MNRAS*, 315, 209
- Kawara, K., et al., 1998, *A&A*, 336, L9
- Lilly S.J., Le Fevre O., Hammer F. & Crampton D., 1996, *ApJL*, 460, L1
- Linden-Vørnle, M.J.D., et al., 2000, *A&A*, 359, 51
- Lutz, D., Spoon, H.W.W., Rigopoulou, D., Moorwood, A.F.M., Genzel, R., 1998 *ApJL* 505, 103
- Lutz, D., Veilleux, S., Genzel, R., 1999, *ApJL*, 517, 13
- Madau et al. 1996 *MNRAS*, 283, 1388
- Matsuhara, H., et al., 2000, *A&A* in press (*astro-ph/0006444*)
- Oliver, S., et al., 2000, *MNRAS* in press (Paper I)
- Oliver, S., Grupponi, C., Serjeant, S., 1998, *MNRAS*, submitted (*astro-ph/9808260*)
- Oort, J.A., 1987, *A&AS* 71, 221
- Oliver, S., 2000, to appear in "Mid- and Far-infrared Astronomy and Future Space Missions", ISAS Report Special Edition (SP No. 14), ed. T. Matsumoto & H. Shibai
- Peacock, J., et a., 2000, *MNRAS*, in press (*astro-ph/9912231*)
- Puget, J.L., 1999, *A&A*, 345, 29
- Rigopoulou, D., Spoon, H.W.W., Genzel, R., Lutz, D., Moorwood, A.F.M., Tran, Q.D., 1999, *AJ*, 118, 2625
- Rowan-Robinson, M., 2000, *ApJ* submitted
- Rowan-Robinson, M., Benn, C.R., Lawrence, A., McMahon, R. G., Broadhurst, T.J., 1993, *MNRAS*, 263, 123
- Rowan-Robinson, M., Helou, G., Walker, D., 1987, *MNRAS* 227, 589
- Rowan-Robinson M. et al., 1997, *MNRAS*, 289, 490
- Sanders, D.B., & Mirabel, I.F., 1996, *Ann. Rev. Astron. Astrop.*, 34, 749
- Saunders, W., Rowan-Robinson, M., Lawrence, A., Efstathiou, G., Kaiser, N., Ellis, R.S., Frenk, C.S., 1990, *MNRAS* 242, 318
- Serjeant, S., 2000, in preparation
- Serjeant, S., Grupponi, C., Oliver, S., 1998, *MNRAS*, submitted (*astro-ph/9808259*)
- Serjeant, S., et al., 2000, *MNRAS* in press (Paper II)
- Smail, I., Ivison, R.J., Blain, A.W., 1997, *ApJ*, 490, L5
- Taniguchi, Y., et al., 1997, *A&A* 328, L9
- Taniguchi, Y., Yoshino, A., Ohyama, Y., Nishiura, S., 1999, *ApJ*, 514, 660
- Telesco, C.M., 1988, *Ann. Rev. Astron. Astrop.*, 26, 343
- Tresse, L., Maddox, S.J., 1998, *ApJ* 495, 691